Potential Modulation on the SCATHA Spacecraft

P. D. Craven*
NASA Marshall Space Flight Center, Alabama
R. C. Olsen[t]
University of Alabama, Huntsville, Alabama
J. Fennell and D. Croley[§]
The Aerospace Corporation, Los Angeles, California
and
T. Aggson[j]
NASA Goddard Space Flight Center, Greenbelt, Maryland

A small (1-V) modulation of the spacecraft potential is observed on the SCATHA satellite through its effects on the data from four instruments: two particle detectors and two field detectors. We show that there is a strong causal link between the modulation of the potential at this 1-V level and a nonuniform distribution of the photoemissive properties of the conducting material on the surface of the satellite.

I. Introduction

A. Satellite Charging

P ROPER analysis of thermal plasma and electric field data from satellites requires an accurate knowledge of the satellite potential. The magnitude of the potential is determined in equilibrium by the requirement that the cur-rents to and from the satellite sum to zero. This includes not only the ambient electron and ion current to the satellite, but also material-dependent currents from the satellite such as those from photoelectrons and secondary electrons. Thus both the plasma environment and the properties of the material on the surface of the satellite play a role in the charging process. Passive control of the potential has been attempted by the careful design and selection of the material used on the satellite, particularly by making the exterior surfaces conductors. This method appears to have been successful on the GEOS-2 satellite in that it did not charge to large potentials.' The potential of GEOS-2 typically floated between +4 and + 10 V.' For particle detectors, a nonzero potential prevents the measurement of the full energy spectrum of the population. This has been an especially bother-some problem for low-energy ion measurements. For example, there is evidence from geosynchronous satellites that positive potentials cause some low-energy populations to be hidden.' However, such populations can be observed if the detector potential is actively controlled.'

For spinning spacecraft, changes in the potential that are phased with the spin period are also a problem in that the flux or count measurements can be highly modulated.[1-5] A spin modulation of the potential distorts the measurements not only of particle detectors but also of field detectors, as will be seen later.

Received Nov. 12, 1985; revision received April 25, 1986.

*Astrophysicist, Space Science Laboratory, Magnetospheric Physics Branch.
[t]Associate Research Professor, Department of Physics.
Senior Scientist, Space Science Laboratory, Particles and Fields Department.
§Member of Technical Staff, Space Science Laboratory.
[j]Research Scientist, Laboratory for Extraterrestrial Physics, Electrodynamics Branch.

It is therefore important to be aware of the existence of a potential modulation. It is also important to know the cause of such modulations so that steps can be taken with future spacecraft to avoid them.

It is the purpose of this paper to report on a small amplitude (~1 V), spin-phased modulation of the potential of the conducting surfaces on the SCATHA satellite and to suggest a possible cause. We will first show the effects of the potential modulation on four instruments—two particle detectors and two field detectors—which are distributed over the satellite. These effects and the positions of the instruments will then be used to show a causal link between the modulation and the properties of the surface materials. The azimuthal variation in the material properties is such that the photoemissive current is modulated. There are two factors that contribute to the modulation of the photoemissive current. One is that the ratio of the illuminated surface area of grounded conductors to insulated surface area varies with the spin. The other is that the photoyield varies for the exposed conductors.

B. SCATHA

The Air Force P78-2 satellite, also known as SCATHA (Spacecraft Charging at High Altitude), was designed to study the causes and dynamics of spacecraft charging, specifically at geosynchronous orbit. The satellite is basically a cylinder approximately 1.75 m in both length and diameter. It is spin stabilized at about 1 rpm with its spin axis in the orbit plane and perpendicular to the Earth-sun line. Many of the instruments are contained in an area around the middle of the cylinder (see Fig. I), the so-called belly band. Both insulating and conducting material are contained in the belly band. Solar cells cover most of the remaining part of the cylinder side. SCATHA is in a nearly geosynchronous orbit with a period of 23.5 h, an apogee of 7.3 *Re*, and a perigee of 5.8 *Re*. A description of the pro-gram and the satellite has been given by Fennell' and Stevens and Vampola.[7]

C. Instrument Description

The four instruments used in this study are the NASA Goddard Space Flight Center electric field monitor (SC10), the Aerospace Corporation sheath field monitor (SC2), the NASA Marshall Space Flight Center light ion mass spectrometer (SC7), and the University of California at San Diego charged particle experiment

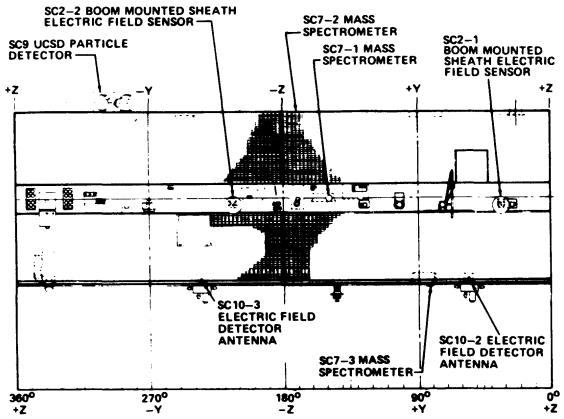

Fig. 1 A plan view of the SCATHA satellite.

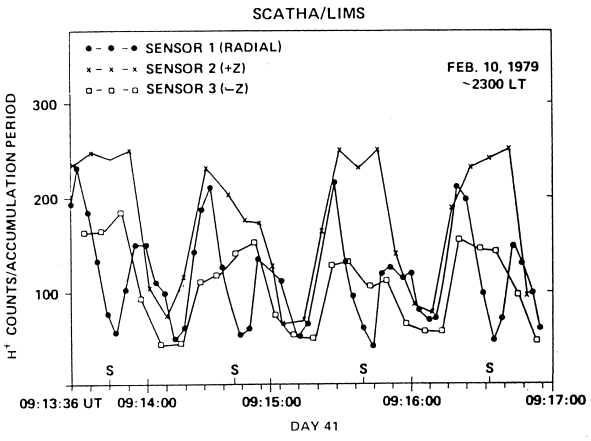

Fig. 2 The effect of the satellite potential change on the LIMS data.

(SC9). The location of each of these instruments is shown in Fig. 1. The designations SC2, SC9, etc., are shorthand notations for each of the instruments on SCATHA. They have no special significance other than for accounting purposes.

The Aerospace Corporation sheath electric field monitor measures the floating potential of two Aquadag (a conductive paint) -coated spheres relative to the spacecraft ground. The spheres have a diameter of about 18 cm and are mounted 3 m from the satellite surface on booms that are 180 deg apart and near the centerline of the satellite. Each sphere has a 25.4-cm-long shadow stub on the side of the spherical probe away from the spacecraft that balances the shadowing effect of the 3-m support booms when the potential difference between the two probes is being measured. This instrument also contains particle detectors, but the data from them are not used here.

The NASA/Goddard electric field detector is a cylindrical double floating ensemble for measuring electric fields. Dipole antennas that are 100 m tip-to-tip in length are used as the floating probes. The antennae wire is composed of beryllium copper. Each of the antennae is insulated except for the last 20 m, which is the active part. Differential signals between the antennas give the ambient electric field. Common mode measurements also made with this instrument give the potential of one probe relative to the spacecraft ground. The data used below are taken from the common mode measurements. The antennas were slowly deployed starting in late February and ending in early March 1979.

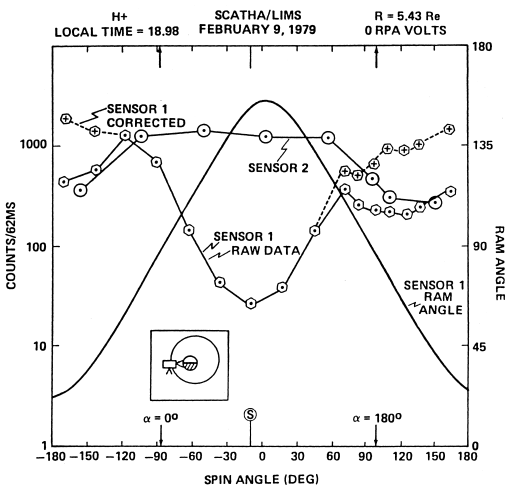

Fig. 3 A plot of H + counts per accumulation period for the LIMS.

The NASA/Marshall light ion mass spectrometer (LIMS) is described in detail by Reasoner et al.[8] A retarding potential analyzer was used in conjunction with a magnetic mass spectrometer to measure the total flux and energy distribution (for energies less than 100 eV) of H+ , He+ , and 0+. There are three sensors associated with this instrument. One views radially from the belly band, one parallel to the spin axis from the forward end of the satellite, and one antiparallel to the spin axis from the aft end. The radial sensor samples a wide range of pitch angles as the satellite spins, while the other two sample pitch angles near 90 deg. All of the sensors operate together, i.e., all are set for the same ion at the same time and all have the same retarding potential at the same time. The output of the radial sensor is sampled twice as often as that of the other two sensors. Each of these sensors is mounted flush with the satellite surface as shown in Fig. I. An electronics failure in the LIMS on February 17, 1979, prior to the deployment of the electric field booms, prevented the acquisition of data simultaneously with the electric field detector.

The University of California at San Diego (USCD) charged-particle experiment is an electrostatic analyzer that measures both ion and electron flux. This instrument, except for the energy range of the detectors, is identical to the UCSD Auroral Particles Experiment on ATS-6.[9] All three of the sensors of this instrument are contained in a single package that is mounted at the forward end of the satellite as shown in Fig. 1. Data shown in the present article are from the sensor that has a radial viewing direction that is fixed relative to the satellite body. The energy range of this sensor is 1 eV to 2 keV with an energy resolution (ΔE/E) of 20%. The angular field of view is 5 x 7 deg. The output of the fixed detector is sampled 8 times/s in the modes used for this work. In order to measure the angular distributions of a given energy ion, the detector dwelled at a fixed energy range for 16 s. The differential measurement characteristics of this instrument complement the integral nature of the LIMS measurements.

II. Observations

A. LIMS

The satellite potential modulation dramatically affects the thermal plasma measurements. This is demonstrated in Fig. 2, which shows the count rates from all three LIMS sensors as a function of time. The radial sensor is looking sunward at the times marked with an S in the figure. All three sensors show a minimum in counts when the sun angle of the radial sensor is about 180 deg.

The LIMS radial sensor (sensor 1) shows a count minimum three times per spin period because there is also an anisotropy in the plasma angular distribution that is not related to the potential modulation. The minimum seen by all of the sensors is not related to the ambient plasma characteristics or to changes of the plasma characteristics but rather is related to changes in the orientation of the spacecraft. Comparisons of this LIMS data with that of the sheath effects monitor during the initial operations of SCATHA showed that both instruments exhibited evidence of a potential change at the same time.[25] Subsequent analysis has shown that the potential modulation effect is also evident in the data from the electric field monitor and the charged particle instrument. The phasing of the modulation in the satellite spin is the same with respect to the sun angle of the +Z axis (the angle between the spacecraft +Z axis and the satellite-sun line) for all the instruments, as will be shown below. The effect is first shown for each of the instruments individually and then as a group.

Figure 3 shows an expanded view of the H+ count rate for the LIMS radial detector (sensor 1) and one of the end detectors (sensor 2), both plotted as a function of the spin angle of sensor 1. The retarding potential analyzer (RPA) is set to zero volts for both sensors. The spin angle is measured from the geocentric equatorial plane and is zero when the LIMS radial sensor's look direction is in the equatorial plane and in the sunward direction. The position of the sun in terms of the spin angle will vary according to the time of the year. For the data in Fig. 3, the angle between the look direction of the radial detector and the satellite sun line is at a minimum at a spin angle of about -15 deg. The S at the bottom of the figure marks this position. The ram angle, the angle between the look direction of the radial sensor and the spacecraft velocity, is plotted in Fig. 3 as the solid line and applies only to the radial sensor. The scale for the ram angle is plotted on the right vertical axis. The inset of this figure shows the look directions of sensor 2 and sensor 1 at the minimum ram angle for this local time position of the satellite. Although the end detector does not change look directions during a spin, the data are plotted against spin angle in order to show the spin-induced variation in the ion count rate. As shown in Fig. 3, which is a typical spin plot for the time frame indicated, there is a plateau in the count rate of sensor 2 from about – 100 to + 60 deg. In general, in the LIMS data from the end sensors during the time periods to be discussed in the following sections, the plateau of up-per counts is found between spin angles of about – 100 to + 75 deg. There is a transition region in which the count rate changes between the upper and lower values. This transition region extends, on average, from +75 to + 110 deg and from – 100 to – 135 deg. Lower count rates are then recorded from + 110 to + 180 and from – 135 to – 180 deg. This transition region is caused by the potential changing to another equilibrium level as a result of materials with different properties becoming illuminated. Since the end sensors do not vary in ram or pitch angles over a spin period, the decrease in the count rate for sensor 2 indicates that the spacecraft potential is changing, becoming more positive.

The uncorrected data from sensor 1 (the solid line) show an angular distribution that might be identified as a pitch angle variation in the absence of other information. The location of the minimum and maximum pitch angles relative to the spin angle is shown by the arrows in Fig. 3. Since the three sensors operate together and are measuring total ion flux (the retarding potential set to zero volts), one can correct, at least to first order, for the potential modulation of the flux into the radial detector by using the data from sensor 2. The ratio of the counts from this sensor in the portion of the curve where the potential is least positive (the plateau) to the counts at a given spin angle is a factor that can be applied to the data from the radial sensor to remove the effects of the potential change during a spin period. Such a correction when applied to this data yields the dashed curve in Fig. 3. The corrected curve shows that the plasma peaks in the ram angle, i.e., where the ram angle is smallest. This indicates an isotropic cold plasma. Energy analysis from the LIMS confirms that the plasma has a cold (kT< 1 eV) component at this time. The difference between the corrected and the uncorrected data in this figure indicates the importance of removing the effects of charging from the data before inferring the basic plasma characteristics. This approach assumes that the flux dependence on the potential and on the ram angle are independent of each other. The work of Comfort et al.[10] suggests that this may not be the case.

B. Aerospace Corporation Sheath Effects Instrument

The sheath effects instrument also shows the effect of a change in the potential during a spin. Figure 4 shows a typical response of the boom-mounted spheres. The sphere voltage measured relative to the spacecraft is plotted as a function of universal time (UT). The vehicle potential modulation is reflected by the change in the common mode voltage from about + 1 to -0.1 V. This change is noted in the center of the figure (from about 16:05:05 to 16:05:25 UT). This modulation is superimposed on the expected variations in the probe voltage caused by variations in the illuminated area of the probes. For each of the spherical probes, a variation in the sun illumination will change the amount of photoemission and that will alter the charge of the probe and therefore its potential relative to the spacecraft. Because of the probe/spacecraft geometry, some spin-related shadowing is expected. This is seen in the response of the probes as the dip in the probe voltage caused by the nonsymmetric shadow of the probe stub (at 16:05:00 UT in Fig. 4 for SC2-2 and 16:05:25 UT for SC2-1), and also as the large decrease caused by the spacecraft's shadowing of the probes. Except for the time in the spacecraft shadow and the nonsymmetric shadow from the probe stub, the illuminated area of the spheres does not change; therefore, the shown decrease in the probe voltage indicates that the spacecraft ground has increased (gone positive relative to the probes). The long electric field antenna had not been deployed at this time but showed similar behavior once deployed.

C. NASA Goddard Electric Field Monitor

The common mode voltage for one of the electric field antennas (SC10-2) is shown in Fig. 5a. Time is plotted along the horizontal axis. The common mode voltage for this instrument is also measured relative to the spacecraft ground. The response of the antennas is similar to the sheath potential probe in that changes in probe illumination cause

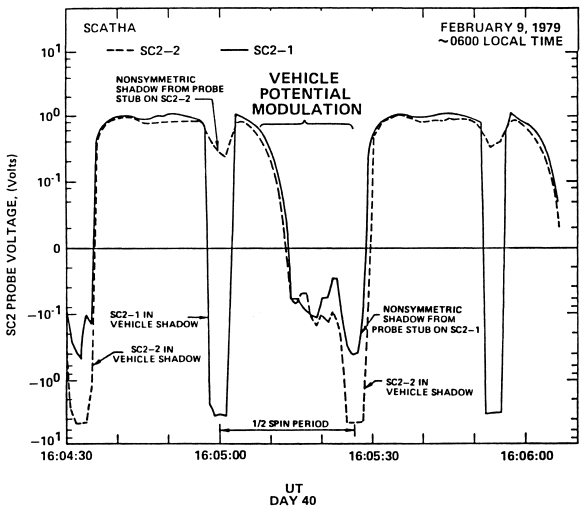

Fig. 4 Atypical potential response of the short booms of the sheath effects monitor.

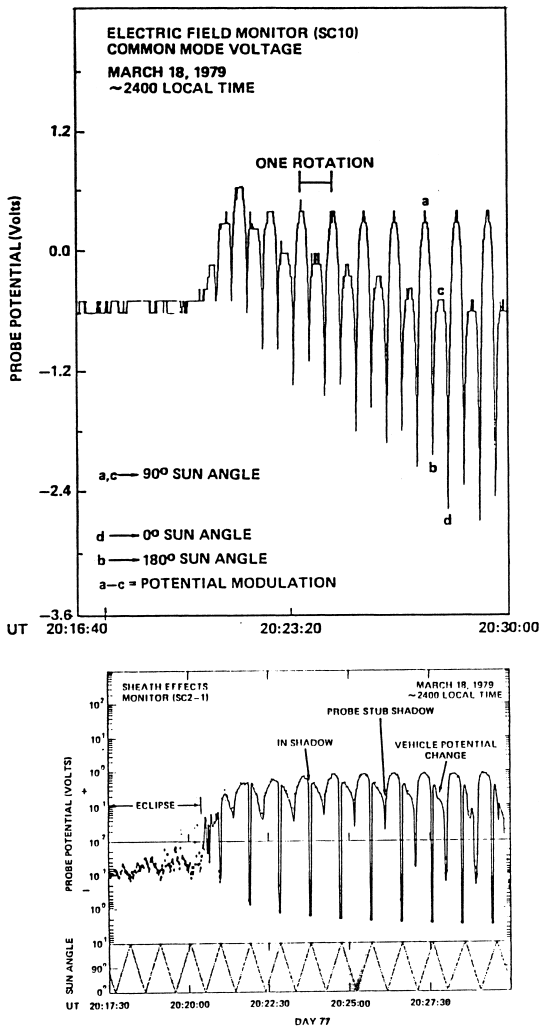

Fig. 5 Response of the field detectors on eclipse exit: a) behavior of the NASA Goddard electric field monitor; b) behavior of the Aerospace Corp. sheath monitor.

changes in photoemission which in turn cause the potential of the antenna relative to the spacecraft ground to vary," The antennas are cylindrical so that the illumination changes drastically with the antennae sun angle, having two positions with grazing incidence illumination (0 and 180-deg sun angle). The antenna sun angle is the angle between the satellite/sun line and a line along the axis of the antennae to the center of the spacecraft. The length of these antennas and their location on the bottom edge of the satellite makes it unlikely that at the 180-deg sun angle they are entirely in the spacecraft shadow. However, the grazing incidence illumination for the cylindrically shaped antennae will appear to have the same effect as an actual blockage of sunlight. This can be seen in Fig. 5a in the positions marked "d" (0-deg sun angle) and "b" (180-deg sun angle). For the angular position at which the sun angle is 90 deg (denoted by "a" and "c" in the figure), there are two distinct levels for each of the extrema of the probe voltages in Fig. 5a. The two maxima differ by approximately a volt after an equilibrium has been reached. The difference in the magnitude of the two maxima results from a change in the spacecraft ground rather than from a difference in the illumination of the antennae." The difference in the minima is probably also caused by the spacecraft potential changes but is not as great because these two points are in the transition phase of the potential.

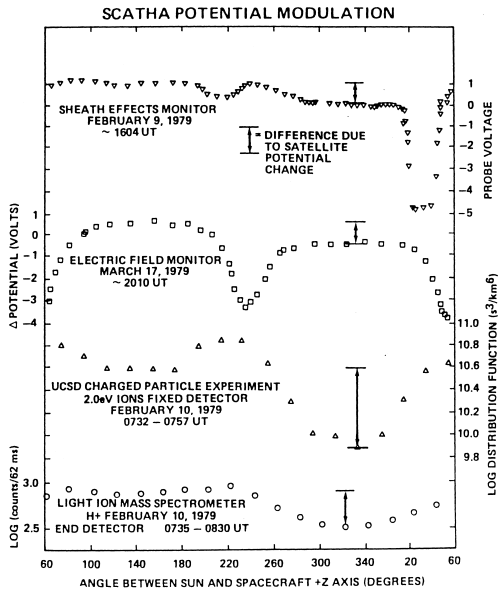

Fig. 6 The modulation cycle of all the instruments plotted as a function of the angle between the +Z axis and the sun.

D. Eclipse

The association of the spin-phased potential modulation with sunlight can be confirmed by examining the behavior of the field detectors (SC2 and SC10) in an eclipse. The pattern of the voltages for the sheath monitor and the electric field probe are shown in Figs. 5a and 5b for exit from an eclipse. Figure 5b plots the potential of the SC2-1 probe and is similar to the plot in Fig. 4, except that the horizontal axis is more compressed. The sun angle of the SC2-1 probe is plotted in the bottom panel of Fig. 5b. (There is an offset of about 23 deg between the SC2-1 probe and the SC10-2 probe, and this is seen in Figs. 5a and 5b.) The transition from the eclipse appears to be abrupt, as seen in Fig. 5b at about 20:21 UT. However, it takes about 5-6 spin periods before the pattern of the probe potential variation is completely re-established. This is about the time that it takes for the solar array current (not shown) to reach a stable value and is indicative of a penumbral effect. However, the asymmetry in the probe potential in the first two spin periods indicates that a spacecraft potential modulation is present at this time and is clearly established by the third spin period. The potential for SC10-2 is shown in Fig. 5a for the same exit from the eclipse as that for SC2-1 in Fig. 5b. The difference in the SC10 probe voltages at perpendicular sun angles slowly increases as the satellite exits eclipse. The reappearance (disappearance) of this pattern of the data for both SC2 and SC10 as the satellite exits (enters) eclipse shows that the modulation in potential for these two probes is related to the sun illumination of a part or parts of the spacecraft. The time needed to establish the patterns at the 1-V level on exiting from the eclipse can largely be attributed to penumbral effects. It is also a result of the time needed to establish a stable periodic potential variation as the spacecraft charges and discharges with some capacitive time constant along with all the isolated surfaces on the satellite.

There are actually two time constants to consider. One is the time constant connected with the potential modulation of the ground potential or mainframe. The other is the time constant for the charging of the whole satellite, including the differential charging of insulated surfaces. Although the satellite potential responds rapidly to changes in the environment or illumination, the

insulating surfaces have a much longer time constant than the grounded conductors. The time constant of the ground potential is shorter than half a spin period since the potential is spin modulated. The level of the potential that is being modulated is also changing but at a much slower rate, on the order of minutes. However, this latter time cannot be easily derived from the data, since penumbral effects and differential charging effects of the spacecraft dielectrics are both present. Differential charging occurs over a time on the order of a minute. Such time constants can be inferred from surface potential monitor experiments on SCATHA.[13]

E. Photosheath

A photoelectron sheath that is asymmetric with respect to the sun direction could affect the instrument measurements. The effects of such a sheath would most easily be seen in the responses of the sheath effects monitor and the electric field monitor. The effect would depend on the size and shape of the photoelectron sheath and would show up as a change in the probe potential as each one rotated in and out of the sheath. Thus for each of these two instruments, the spin-related behavior of the common mode voltage should be the same for each probe except for the phase. Examination of the March 18, 1979, (day 77) data from the two field monitor instruments shows that all four probes simultaneously change in the same way. This change occurs for all the probes (actually all four instruments) at the same UT. This simultaneous change indicates that this part of the response of the probes is caused by the modulation of the spacecraft ground and not by a photoelectron sheath. Furthermore, since the sheath monitor should be well within the spacecraft sheath and the electric field monitor outside it or on the edge[12] the small difference in the shapes of the curves at sun angles other than 0 or 180 deg (see Fig. 6) shows that the sheath effect on the probe response for both of the instruments is, on this day, small in comparison to the change in the spacecraft ground.

F. Summary of Observations

In order to pinpoint which part 'or parts of the spacecraft when illuminated are causing the spacecraft potential to be modulated, we plotted the modulation cycle for each of the instruments as a function of the angle between the spacecraft + Z axis and the spacecraft/sun line. This plot is shown in Fig. 6. The angle between the spacecraft + Z axis and the sun is plotted along the horizontal axis. The figure axis does not start at zero in order to show clearly the two parts of the modulation cycle. The probe voltage on the vertical axis for the two field detectors is a linear scale while the particle detector axis is a log scale, reflecting the expected effects of a potential on the two types of detectors. From this figure, it is evident that all four instruments are responding to the effects of a change in spacecraft potential at the same time. The cycle is such that the potential is at a maximum when the angle between the sun and the + Z axis is between 260 and 20 deg. A radial vector from the satellite to the sun in the center of this minimum passes very near the SC9 position.

III. Analysis

It is expected that the sun's illumination is a dominant factor in determining the spacecraft potential, since at the geosynchronous orbit the photocurrent is the major current from the spacecraft.14,'5 Changes in the plasma temperature were not observed by either of the particle instruments on February 9 and 10, 1979, during the time the potential modulation is evident. This combined with the strong coup-ling between the spacecraft spin period and the changes in the count rates of the two particle instruments makes it unlikely that the spacecraft is responding to a change in plasma densities. Therefore, the change must be related entirely to sun

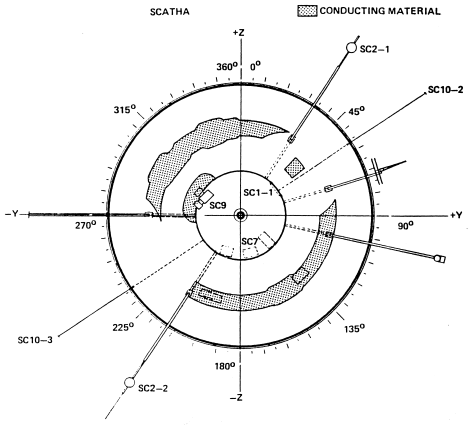

Fig. 7 The distribution of grounded conducting exterior surfaces on SCATHA.

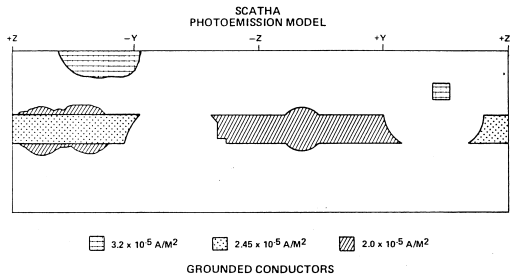

Fig. 8 A plot of the photoemissive yield model of SCATHA used to calculate the total photocurrent.

illumination or more exactly to photoemission. Surface material properties are therefore suspect, especially those materials that are likely to influence the spacecraft ground potential. Since conducting surfaces are tied to the spacecraft frame, a close examination of them is in order. The normal to the ends of the satellite are kept perpendicular to the sun within ±5 deg so that the materials on the for-ward and aft ends will not contribute significantly to the spacecraft charge, at least not through photoemission. The surface of the cylinder is mostly covered with insulating materials (e.g., solar cells). The distribution of the conducting material on the cylinder surface is shown in Fig. 7, in which the entire satellite is drawn in the same plane. The angles in this figure increase in the direction of sun movement relative to the satellite (opposite to satellite rotation) and are measured from the +Z axis. Most of the conducting material is contained in the band around the middle of the cylinder that contains the instruments. However, there is a significant area of indium oxide (a conductor) on the solar cells under the SC9 instrument.

In addition to knowing the position and area of the con-ducting material, one must also know the photoemissive properties of the materials. We used the same photoemissive values for the materials as used by Stannard et al.[16] in an analysis of SCATHA charging. The model of the conductive surfaces photoemissive yield for normal incidence used in this study is shown in Fig. 8. Unless noted otherwise in the figure, the surface materials (both the conductors and the insulators) have a photoelectron yield of 2×10^{-5} A/m^2 for normally incident sunlight. The photoemissive yield of 2.45×10^{-5} A/m^2 shown in Fig. 8 for part of the belly band is the average yield of alternating stripes of gold and yellow conducting paint.

In order to show the connection between photoemission and the change in the spacecraft potential, we assumed the spacecraft potential to be zero and calculated the total photocurrent from the grounded conducting materials on the satellite as a function of the angle from the spacecraft + Z axis. For this purpose, the cylindrical surface was divided into 10-deg bands, and the photocurrents from the different conducting materials in each 10-deg band were summed. The total photocurrent resulting from a particular orientation of the satellite was calculated by integrating the photocurrents from each band weighted by the cosine of the angle from the band to the sun. This assumes no change in the photoemissive yield, except for the decrease in area for off normal incidence. When a particular band faced the sun directly, the photocurrent from it contributed to the integral with no reduction, while those bands on either side and 90 deg or greater from the center band, i.e., 90 deg from the sun, contributed nothing to the integral.

This total photocurrent from the illuminated grounded conducting material is plotted in Fig. 9 as a function of the angle between the sun/satellite line and the + Z axis. The total photocurrent is plotted on the left-hand scale. Counts from the LIMS sensor 2 that have been averaged over about 60 consecutive spins, are also shown. The LIMS counts are plotted on the right-hand scale. A distinct asymmetry in the photocurrent is shown. The photoemissive current from the satellite is greatest near the indium oxide coating under the UCSD instrument. The large peak in the calculated photocurrent seen at this point is the result of a combination of increasing conducting area and increasing photomissive yield. A smaller peak in the photocurrent is evident at about 140 deg, also coinciding with a decrease in the LIMS counts from sensor [2]. There is good agreement between the change in the photoemissive current and the potential cycle exhibited by the four instruments and represented by the LIMS data. It does not appear that the potential modulation is caused by an angular anisotropy of the electrons or ions." The evidence for this comes from the fact that neither the ions nor the electrons are coming predominantly from one direction or the other when trapped or field-aligned. Since there are not two peaks per spin period in any of the instruments, the angular anisotropy in the particles is not causing the potential modulation reported on here. Ram effects can also be ruled out by noting that the ram angle varies with local time, being on the forward end of the spacecraft at local midnight and the aft end at local noon, and that the potential modulation has been seen at dusk, dawn, and near local midnight. At local midnight, the surfaces do not rotate into and out of the ram direction. It thus appears that the small potential change experienced by the SCATHA satellite is caused by a nonuniform distribution of the material proper-ties of the grounded conductors on the satellite. Both the insulators and the conductors experience photoemission, and electrons emitted by one can be collected by the other. The fact that the effects of the potential change reported on here are strongly linked to conducting materials is a result of the conductors being grounded directly to the spacecraft frame.

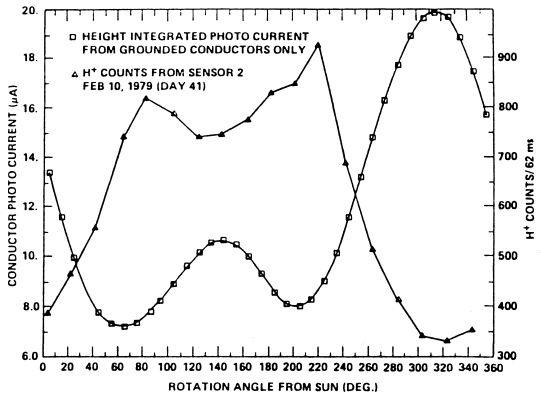

Fig. 9 The total photocurrent of illuminated grounded exterior conducting surfaces as a function of the angle between the spacecraft + Z axis and the sun.

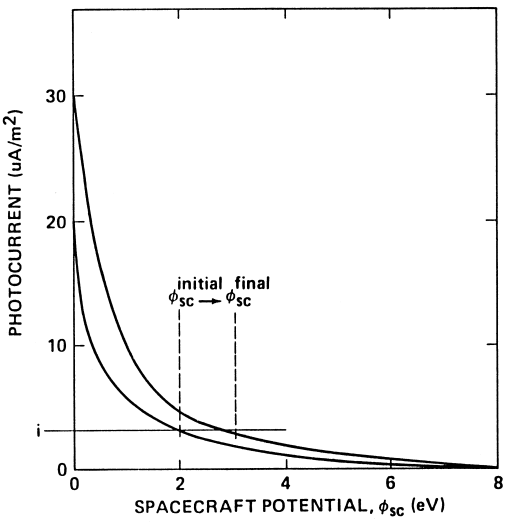

Fig. 10 A representation of the photocurrent from a surface as a function of the potential of the surface.

IV. Conclusions

We have shown that small potential changes can be experienced during the spin period of a spacecraft. The potential modulation observed on SCATHA is dominated by a nonuniform distribution of the photoemissive properties of the exposed conducting materials that are directly grounded to the spacecraft frame and of the area of these materials. It does not appear that the phenomenon reported on here is a result of differential charging and a corresponding charging of the spacecraft as reported for ATS-6 by Olsen and Purvis.10 The surfaces that are responsible for the potential change on SCATHA are grounded to the spacecraft frame and should not differentially charge. Further evidence that the effect is not caused by differential charging is seen in the response of the two types of instruments. The field instruments see the effect as a change in the spacecraft ground. The particle instruments see the modulation as a change in the potential of the surface near the detectors. Since all the instruments respond to the change in the same way and at the same time, it appears that the spacecraft ground and the potential of the grounded conductors are changing at the same time and in the same way even though the conductors are distributed around the surface of the satellite.

In the analysis of the photocurrent above, the spacecraft potential was assumed to be zero. The photocurrent will be affected by a potential on the spacecraft in that the photoelectrons will be attracted to the spacecraft if the potential is positive and repelled if the potential is negative. In order for the potential to change while the ambient cur-rent remains the same, the escaping photocurrent must change. This occurs if the number of electrons in the tail of the distribution function increases. This behavior is shown schematically in Fig. 10. This figure is a plot of a surface's current density caused by photoemission vs the potential of the

surface. If the ambient current to the satellite is as shown in the figure, then as a material with a greater photocurrent rotates into the sun, the satellite ground will change levels as necessary to maintain a zero net current. In general, it will become more positive as shown in the figure. This interpretation is based on the data of Grard[19] and Feuerbacher and Fitton.[20]

The modulation is easily seen when the potential of the spacecraft is apparently small, i.e., on the order of several volts. The density and temperature of the ion population measured by both the light ion mass spectrometer and the UCSD instrument on February 9 and 10, 1979,and by the UCSD instrument on March 18, 1979, (day 77) indicate that the satellite is in the outer plasmasphere during the times that the modulation is most obvious. Since the cause of the modulation is ultimately the sun's illumination, it must surely be present at other times (excluding eclipse) when the satellite is outside the plasmapause. This affect will be reduced if the satellite potential is highly positive (> 10 eV), since then most of the photoelectrons are trapped. This is a regime where the plasma population has a higher temperature, and in this case, a 1-V potential modulation would not be obvious in the particle data.

For the same satellite, a different spin rate would probably not affect the results given here. The reason is that the 1-V potential modulation appears to be driven mainly by the grounded conductors and not the dielectrics. The grounded conductors can respond in times on the order of milliseconds,21 whereas the dielectrics (insulators) charge over a time period on the order of minutes,13•14 so even rapid spin rates would probably not affect the results. At lower spin rates, 1 rpd say, the effect would probably be masked by other events such as a change in the ambient plasma.

The avoidance of small potential modulations such as reported here is particularly important for low energy particle measurements. Thus, when such measurements are to be made on a spinning spacecraft that is to have passive electrostatic control, an attempt should be made to balance the material properties related to photoelectron emission. However, since it seems unlikely that material properties will be known well enough to avoid completely small potential modulations through passive control, other methods should be considered. One such method is active control of the spacecraft potential using plasma emitters.[22, 23]

Appendix

The spin modulation of the potential of the electric field antennae provides a piece of information that could be quite useful for experimenters on future satellites. When the antenna is pointed toward the sun, it is effectively in eclipse; hence the drop in potential as seen, for example, in Fig. 5a. The difference between the potential of the antenna in eclipse and in sunlight provides a measure of the floating potential of the satellite mainframe in sunlight. On March 18, 1979, (day 77) the antenna potential shows a spin modulation of 2 or 3 V (from +0 or +1 to -2 V, with respect to the mainframe). On this day as the satellite enters eclipse, the antennae potential attains a constant value of nearly zero volts with respect to the satellite. This means that in eclipse, the antenna potential and satellite potential are the same. If the antenna potential while end-on to the sun is indeed the eclipse potential of the antenna, then the modulation in the antenna potential provides a measure of the difference between sunlight and eclipse satellite potentials. Since the floating potential of the satellite in an eclipse is not zero, the antennae potential only provides a relative measurement. This can still be a useful element in the analysis of satellite data. In addition, other instruments on future satellites could make use of such data. In particular, aperture bias techniques, such as those used on the Dynamics Explorer 1 Retarding Ion Mass Spectrometer,[24] would benefit from this type of feedback.

Acknowledgments

The authors would like to note that Sherman DeForest was the Principal Investigator for the UCSD instrument and that C. R. Chappell was the Principal Investigator for the LIMS. We would like to thank C. E. Mcllwain for sending us the UCSD instrument data that was used in this paper. J. Fennell and D. Croley were partially supported for this work by the Air Force Systems Command Space Division under Contract F04701-85-C-0086; R. C. Olsen was partially supported by NASA under Contract NAS8-33982.

References

[1]Knott, K., Decreau, P. M. E., Korth, A., Pedersen, A., and Wrenn, G. L., "The Potential of an Electrostatically Clean Geostationary Satellite and Its Use in Plasma Diagnostics," *Planetary Space Science, Vol.* 32, Feb. 1984, pp. 227-237.

[2]Olsen, R. C., "The Hidden Ion Population in the Magnetosphere," *Journal of Geophysical Research,* Vol. 87, May 1982, pp. 3481-3488.

[3]Sojka, J. J., Wrenn, G. L., and Johnson, J. F. E., "Pitch Angle Properties of Magnetospheric Thermal Protons and Satellite Sheath Interference in Their Observation," *Journal of Geophysical Research,* Vol. 89, Nov. 1984, pp. 9801-9811.

[4]DeForest, S. E. and Mcllwain, C. E., "Plasma Clouds in the Magnetosphere," *Journal of Geophysical Research,* Vol. 76, June 1971, pp. 3587-3611.

[5]DeForest, S. E., "Electrostatic Potentials Developed by ATS-5," *Photon and Particle Interactions With Surfaces in Space,* edited by R. J. L. Grard, D. Reidel Publishing Company, Dordrecht, The Netherlands, 1973, pp. 263-276.

[6]Fennell, J. F., "Description of the P78-2 (SCATHA) Satellite and Experiments," *The IMS Source Book,* edited by C. T. Russell and D. J. Southwood, American Geophysical Union, Washington, DC, 1982, pp. 65-81.

[7]Stevens, J. R. and Vampola, Al. L. (eds.), "Description of the Space Test Program P78-2 Spacecraft and Payloads," Space and Missile Systems Organization, Los Angeles, CA, Tech. Rept. SAMSO TR-78-24, 1978.

[8]Reasoner, D. L., Chappell, C. R., Fields, S. A., and Lewter, W. J., "Light Ion Mass Spectrometer for Space Plasma Investigations," *Review of Scientific Instruments,* Vol. 53, April 1982, pp. 441-448.

[9]Mauk, B. H. and McIlwain, C. E., "ATS-6 Auroral Particles Experiment," *IEEE Transactions on Aerospace and Electronics Systems,* AES-11, Nov. 1975, pp. 1125-1130.

[1°]Comfort, R. H., Baugher, C. R., and Chappell, C. R., "Use of the Thin Sheath Approximation for Obtaining Ion Temperatures from the IEEE 1 Limited Aperture RPA," *Journal of Geophysical Research,* Vol. 87, July, 1982, pp. 5109-5123.

"Lai, S. T. and Cohen, H. A., "Boom Potential of a Rotating Satellite in Sunlight," EOS (Abstract), Vol. 65, April 1984, p. 261.

[12]Aggson, T. L., Ledley, B. D., Egel, A., and Katz, I., "Probe Measurements of DC Electric Fields," Proceedings of the 17th ESLAB Symposium on Spacecraft/Plasma Interactions and Their Influence on Field and Particle Measurements, Noordwijk, The Netherlands, ESA SP-198, 1983, pp. 13-17.

[13]Mizera, P. F., "Charging Results from the Satellite Surface Potential Monitor," *Journal of Spacecraft and Rockets, Vol.* 18, Nov.-Dec. 1981, pp. 506-509.

[14]Knott, K., "The Equilibrium Potential of a Magnetospheric Satellite in an Eclipse Situation," *Planetary Space Science, Vol.* 20, Aug. 1972, pp. 1137-1146.

[15]Grard, R., Knott, K., and Pedersen, A., "Spacecraft Charging Effects," *Space Science Reviews,* Vol. 34, March 1983, pp. 289-304.

[16]Stannard, P. R. et al., "Analysis of the Charging of the SCATHA (P78-2) Satellite," NASA CR-165348, 1980.

[17]Fennell, J. F., Croley, D. R. Jr., Mizera, P. F., and Richardson, J. D., "Electron Angular Distributions During Charging Events," *Spacecraft Charging Technology 1980,* NASA Conference Publication 2182 (AFGL-TR-81-0270), 1981, pp. 370-385.

[18]OIsen, R. C. and Purvis, C. K., "Observations of Charging Dynamics," *Journal of Geophysical Research,* Vol. 88, July 1983, pp. 5657-5667.

[19]Grard, R. J. L., "Properties of the Satellite Photoelectron Sheath Derived from Photoemission Laboratory Measurements," *Journal of Geophysical Research,* Vol. 78, June 1973, pp. 2885-2906.

[20]Feuerbacher, B. and Fitton, B., "Experimental Investigation of Photoemission from Satellite Surface Material," *Journal of Applied Physics,* Vol. 43, April 1972, pp. 1563-1572.

[21] Katz, I., Parks, D. E., Wang, S., and Wilson, A., "Dynamic Modeling of Spacecraft in a Collisionless Plasma," *Proceedings of the Spacecraft Charging Technology Conference,* edited by C. P. Pike and R. R. Lovell, NASA Lewis Research Center, Cleveland, OH, NASA TMX-73537 (AFGL-TR-77-0051), 1977, p. 319.

[22]Olsen, R. C., "Modification of a Spacecraft Potential by Plasma Emission," *Journal of Spacecraft and Rockets,* Vol. 18, Sept.-Oct. 1981, pp. 462-469.

[23]Pedersen, A., Chappell, C. R., Knott, K., and Olsen, R. C., "Methods for Keeping a Conductive Spacecraft Near the Plasma Potential," Proceedings of the 17th ESLAB Symposium on Spacecraft/Plasma Interactions and Their Influence on Field and Particle Measurements, Noordwijk, The Netherlands, ESA SP-3198, 1983. pp. 185-190.

[24]Olsen, R. C., Gallagher, D. L., Chappell, C. R., Green, J. L., and Shawhan, S. D., "A Potential Control Method for Thermal Plasma Measurements on the DE-1 Spacecraft," *Proceedings of the 17th ESLAB Symposium on Spacecraft/Plasma Interactions and Their Influence on Field and Particle Measurements,* Noordwijk, The Netherlands, ESA SP-198, 1983, op. 177-184.

[25]Reasoner, D.L., private communication, Huntsville, AL, 1979.